NDT-NDE Crack Characterization Through a Learning-by-Examples Approach

M. Salucci, N. Anselmi, G. Oliveri, and A. Massa

Abstract

This document deals with the characterization of a single narrow crack in a planar conductive structure starting from eddy current testing (*ECT*) measurements. More precisely, the inversion problem at hand is formulated within the so-called learning-by-examples (*LBE*) paradigm, by considering the problem of estimating the dimensions of the defect as a regression one. Accordingly, a set of known input-output pairs is generated during an *off-line* phase and is given as input to a Support Vector Regressor (*SVR*) prediction model in order to train it on the relationship between defect and corresponding *ECT* data. Some numerical results are shown in order to verify the effectiveness, as well as the limits, of the proposed *LBE* technique when dealing with the presence of noise on testing data during the *on-line* inversion phase.

1 Crack Dimensions Estimation Inside a Plate Structure

1.1 Description

Let be given an homogeneous plate of thickness T and conductivity σ affected by a narrow crack and inspected by a single coil working in absolute mode at frequency f with lift-off δ (Fig. 1). The dimensions of the crack are completely described by the vector $\mathbf{p}$ of $I = 3$ parameters

$$\mathbf{p} = \{d_0, l_0, w_0\} \tag{1}$$

which correspond to its depth, length and width, respectively. Moreover, we assume that the location of the crack (identified by the triplet of coordinates (x_0, y_0, z_0)) is fixed and known (Fig. 1).

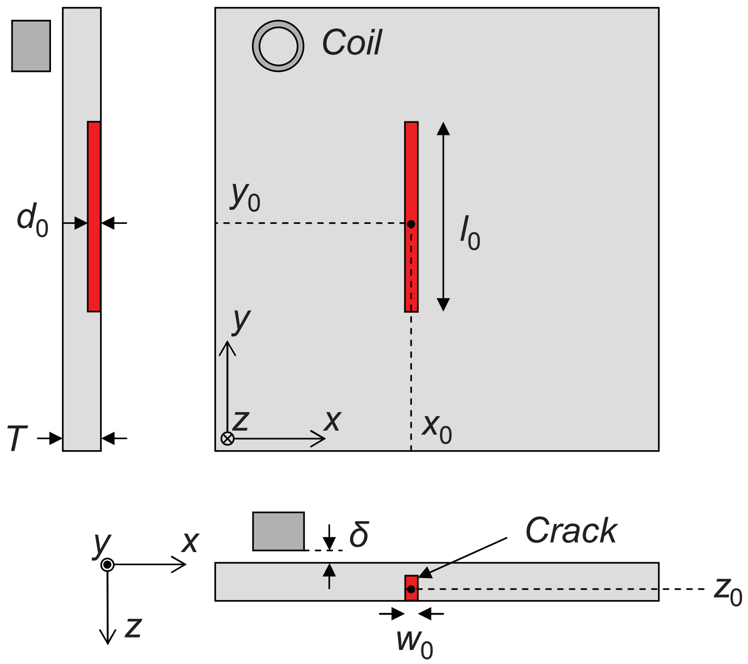

Figure 1: Geometry of the problem.

A metamodel is used as forward solver to compute in a fast but accurate way the measured *ECT* signal associated to a particular dimension of the defect. More in details, for a given vector $\mathbf{p}$ of crack descriptors, the metamodel computes the complex *ECT* signal over a set of K measurement points uniformly distributed on the (x, y) plane

$$\mathbf{\Psi} = \Phi\{\mathbf{p}\} = \{\Psi_k;\, k = 1, ..., K\} \tag{2}$$

where

- $\Psi_k = \Re\{\Psi_k\} + j\Im\{\Psi_k\}$ is the complex-valued *ECT* signal collected by the k-th measurement point (i.e., the impedance variation on the coil);

- $\Phi\{.\}$ is the forward operator, linking the defect barycentre ($\mathbf{p}$) to the collected *ECT* signal ($\mathbf{\Psi}$).

The goal of the inverse problem is to retrieve an estimation of the (unknown) dimensions of the flaw $\widetilde{\mathbf{p}} = \left\{\widetilde{d}_0, \widetilde{l}_0, \widetilde{w}_0\right\}$ (i.e., the output space) by exploiting the information embedded inside $\mathbf{\Psi}$ (i.e., the input space). Such a problem can be formulated as follows

$$\widetilde{\mathbf{p}} = \Phi^{-1}\{\mathbf{\Psi}\} \tag{3}$$

where $\Phi^{-1}\{.\}$ denotes the (unknown) inverse operator, that has to be estimated.

1.2 Parameters of the forward solver (fixed)

- **Forward solver**
  - total number of measurement points along x (i.e., across the crack): $H_x = 41$;
  - measurement step along x: $\Delta_x = 0.5$ [mm];
  - total extension of the measurement region along x: $L_x = 20.0$ [mm];
  - total number of measurement points along y (i.e., along the crack): $H_y = 57$;
  - measurement step along y: $\Delta_y = 0.5$ [mm];
  - total extension of the measurement region along y: $L_y = 28.0$ [mm];
  - total number of measurement point computed by the forward solver: $H = H_x \times H_y = 2337$;

Plate	
Thickness T	1.55 [mm]
Conductivity σ	1.02 [MS/m]
Coil	
Inner radius r_1	1.0 [mm]
Outer radius r_2	1.75 [mm]
Length l_c	2.0 [mm]
Number of turns n_t	328
Lift-off δ	0.303 [mm]
Frequency f	100.0 [KHz]
Crack	
x-Coordinate x_0	15.0 [mm]
y-Coordinate y_0	15.0 [mm]
z-Coordinate z_0	1.24 [mm]

Table 1: Fixed parameters.

Parameter	Min [mm]	Max [mm]
Crack Depth d_0	0.31	1.24
Crack Length l_0	5.0	20.0
Crack Width w_0	0.05	0.4

Table 2: Validity ranges of the forward meta-model.

1.3 Standard LBE Approach ($GRID - SVR$): Performances

1.3.1 Parameters

- **Measurement set-up for the inversion**
  - considered measurement step: $\Delta_x = \Delta_y = 0.5$ [mm];
  - number of considered measurement points $K = K_x \times K_y = 5 \times 31 = 155$;
  - measured quantity for each k-th point: $\{\Re(\Psi_k), \Im(\Psi_k)\}$;
  - total number of measured features: $F = 2 \times K = 310$;

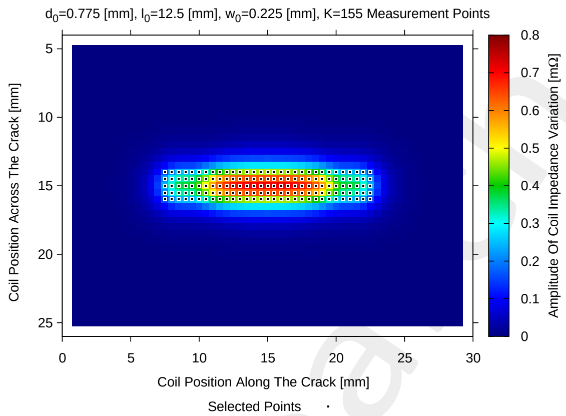

Figure 2: Location of the measurement points selected for the inversion ($K = 155$).

- **Standard LBE Approach**
  - Training set generation
    - sampling: uniform grid sampling in (d_0, l_0, w_0);
    - number of quantization levels: $Q_{x_0} = Q_{y_0} = Q_{z_0} = \{5; 6; ...; 10\}$;
    - number of training samples: $N = Q_{x_0} \times Q_{y_0} \times Q_{z_0} = \{125; 216; ...; 1000\}$;
    - SNR on training data: Noiseless;
  - Test set generation
    - Sampling: Latin Hypercube Sampling (LHS);
    - Number of test samples: $M = 1000$;
    - SNR on test data: Noiseless + $SNR = \{40; 30; 20; 10\}$ [dB].

1.3.2 Calibration of the SVR parameters via cross-validation

The best (C, γ) pair of parameters is selected for training the three SVR regressors.

Parameters

- number of subsets: $V = 5$;
- variation range for parameter C: $C \in \{10^0; 10^1; ...; 10^6\}$;
- variation range for parameter γ: $\gamma \in \{10^{-5}; 10^{-5}; ...; 10^0\}$;
- dimension of the training set: $N = 1000$;

Results

Parameter	**Best** C $(C*)$	**Best** γ $(\gamma*)$	**CV MSE** (η)
Crack Depth d_0	10^3	10^{-3}	2.12×10^{-3}
Crack Length l_0	10^4	10^{-2}	4.53×10^{-3}
Crack Width w_0	10^6	10^{-4}	2.34×10^{-3}

Table 3: Optimal (C, γ) pairs and CV MSE found by applying a 5-fold cross-validation for the estimation of the crack dimensions.

1.3.3 True vs. Predicted ($SNR = 20$ [dB])

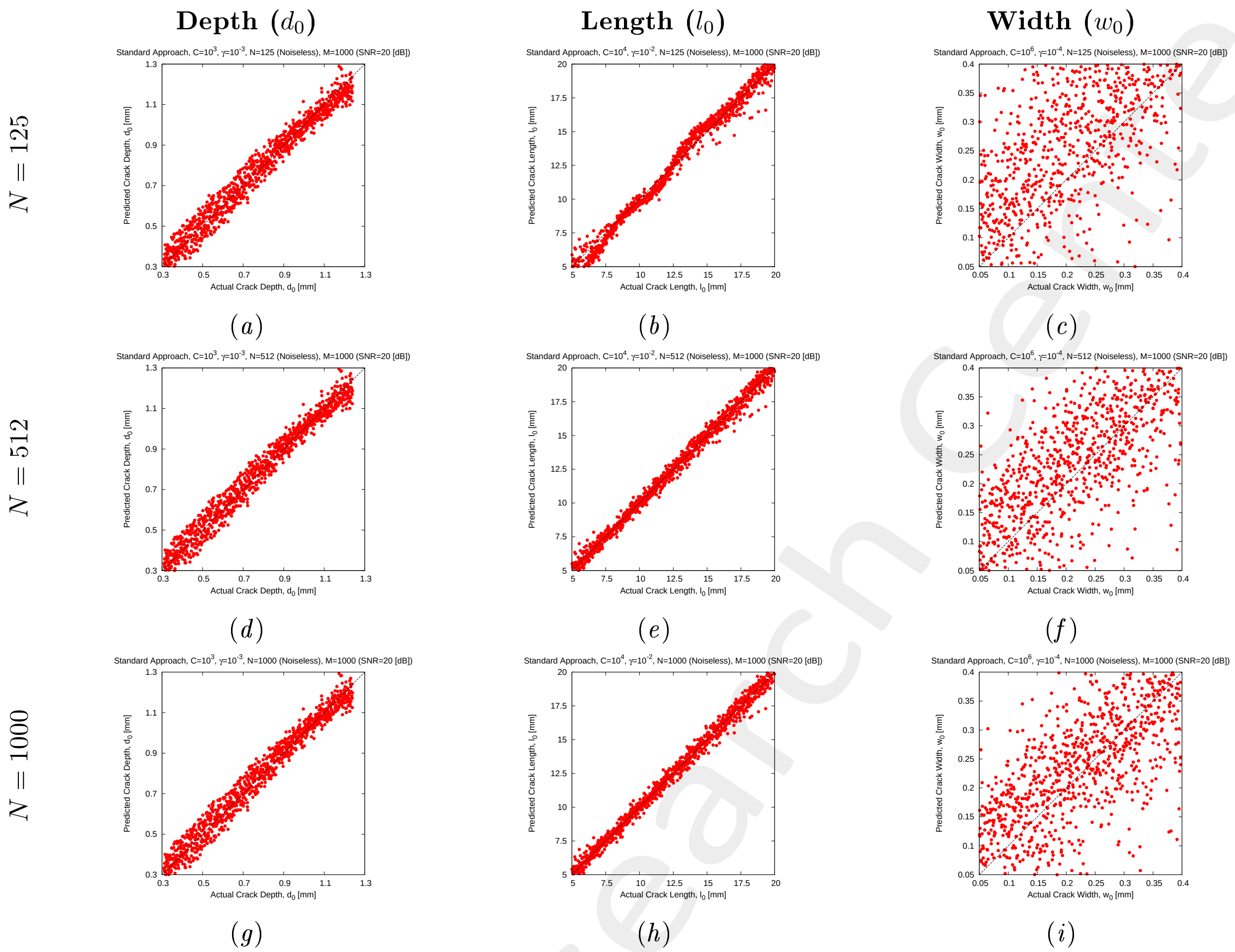

Figure 3: **Standard Approach -** True vs. predicted crack dimensions for different dimensions of the training set (N). $SNR = 20$ [dB] on test ECT data.

1.3.4 Prediction Errors

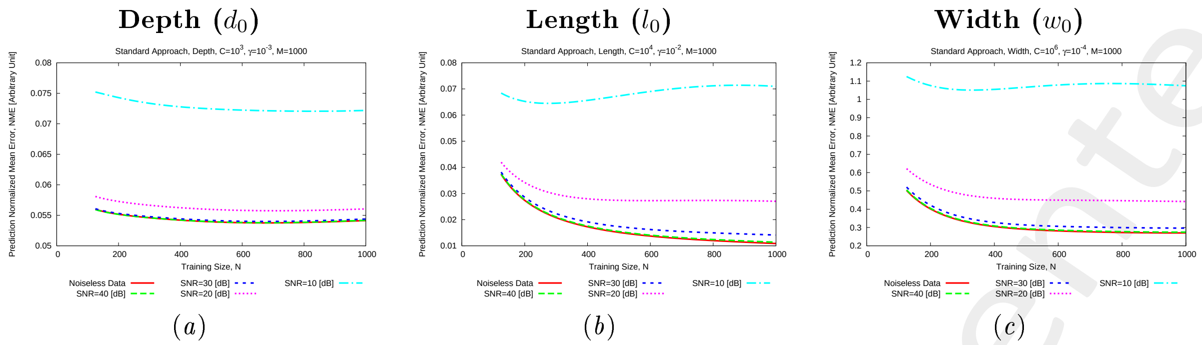

Figure 4: **Standard Approach** - Normalized Mean Error (NME) vs. training size (N)

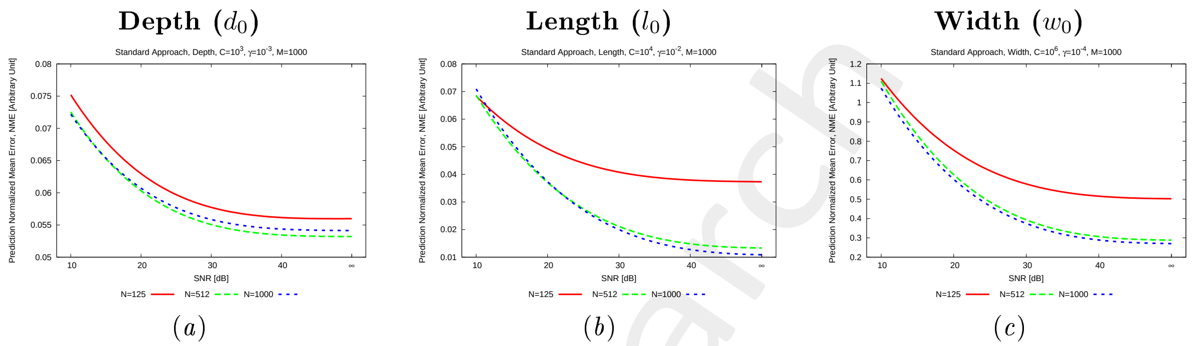

Figure 5: **Standard Approach** - Normalized Mean Error (NME) vs. SNR on the test ECT measurements.

More information on the topics of this document can be found in the following list of references.

References

[1] M. Salucci, N. Anselmi, G. Oliveri, P. Calmon, R. Miorelli, C. Reboud, and A. Massa, “Real-time NDT-NDE through an innovative adaptive partial least squares SVR inversion approach," *IEEE Trans. Geosci. Remote Sens.*, vol. 54, no. 11, pp. 6818-6832, Nov. 2016.

[2] M. Salucci, G. Oliveri, F. Viani, R. Miorelli, C. Reboud, P. Calmon, and A. Massa, “A learning-by-examples approach for non-destructive localization and characterization of defects through eddy current testing measurements," *in 2015 IEEE International Symposium on Antennas and Propagation, Vancouver, 2015*, pp. 900-901.

[3] M. Salucci, S. Ahmed and A. Massa, “An adaptive Learning-by-Examples strategy for efficient Eddy Current Testing of conductive structures," *in 2016 European Conference on Antennas and Propagation*, Davos, 2016, pp. 1-4.

[4] P. Rocca, M. Benedetti, M. Donelli, D. Franceschini, and A. Massa, “Evolutionary optimization as applied to inverse problems," *Inverse Probl.*, vol. 25, pp. 1-41, Dec. 2009.

[5] A. Massa, P. Rocca, and G. Oliveri, “Compressive sensing in electromagnetics - A review," *IEEE Antennas Propag. Mag.*, pp. 224-238, vol. 57, no. 1, Feb. 2015.

[6] N. Anselmi, G. Oliveri, M. Salucci, and A. Massa, “Wavelet-based compressive imaging of sparse targets," *IEEE Trans. Antennas Propag.*, vol. 63, no. 11, pp. 4889-4900, Nov. 2015.

[7] M. Salucci, G. Oliveri, and A. Massa, “GPR prospecting through an inverse-scattering frequency-hopping multifocusing approach," *IEEE Trans. Geosci. Remote Sens.*, vol. 53, no. 12, pp. 6573-6592, Dec. 2015.

[8] T. Moriyama, G. Oliveri, M. Salucci, and T. Takenaka, “A multi-scaling forward-backward time-stepping method for microwave imaging," *IEICE Electron. Express*, vol. 11, no. 16, pp. 1-12, Aug. 2014.

[9] T. Moriyama, M. Salucci, M. Tanaka, and T. Takenaka, “Image reconstruction from total electric field data with no information on the incident field," *J. Electromagnet. Wave.*, vol. 30, no. 9, pp. 1162-1170, 2016.

[10] M. Salucci, L. Poli, and A. Massa, “Advanced multi-frequency GPR data processing for non-linear deterministic imaging," *Signal Processing*, vol. 132, pp. 306-318, Mar. 2017.